Applied Soft Computing 130 (2022) 109685

Contents lists available at ScienceDirect

Applied Soft Computing

journal homepage: www.elsevier.com/locate/asoc

MI-EEG classification using Shannon complex wavelet and convolutional neural networks

Chang Wang [a,b,c,d], Yang Wu [a,c,d], Chen Wang [a,c,d], Yu Zhu [a,c,d], Chong Wang [a,c,d], Yanxiang Niu [a,c,d], Zhenpeng Shao [a,c,d], Xudong Gao [a,c,d], Zongya Zhao [a,c,d], Yi Yu [a,c,d,*]

[a] College of Medical Engineering, Xinxiang Medical University, Xinxiang 453003, China
[b] The Third Affiliated Hospital of Xinxiang Medical University, Xinxiang 453003, China
[c] Henan Engineering Technology Research Center of Neurosensor and Control, Xinxiang 453003, China
[d] Xinxiang Engineering Technology Research Center of Intelligent Medical Imaging Diagnosis, Xinxiang 453003, China

ARTICLE INFO

Article history:
Received 15 March 2022
Received in revised form 10 August 2022
Accepted 23 September 2022
Available online 7 October 2022

Keywords:
Motor imagination
EEG signals
Convolutional neural networks
Shannon complex wavelet
Classification accuracy

ABSTRACT

Many classification methods by machine learning and convolutional neural networks (CNN) have been proposed to recognize MI-EEG recently. However, the indescribable properties and individual differences of the MI-EEG signals cause low classification accuracy. In this study, a new MI-EEG classification method was designed to improve classification accuracy by combining Shannon complex wavelets and convolutional neural networks. First, the original MI-EEG was preprocessed using EEGLAB by channel selection and bandpass filtering. Second, the Shannon complex wavelet was used as the time–frequency transform strategy to calculate the time–frequency matrix. Finally, an improved Resnet was used to classify the time–frequency matrix to complete the MI-EEG identification. BCI competition IV dataset 2b as a public motor imagination dataset was tested to prove the validation of this proposed method. The classification accuracy and kappa value were adopted to prove the superiority of the proposed method by comparing it with the state-of-the-art classification methods. Experimental results showed that the classification accuracy and kappa values are 0.852 and 0.704, respectively, and they are the highest in the state-of-the-art. The parameter influence of wavelet wavelength and interception time on classification accuracy was discussed and optimized. This method can effectively improve classification accuracy and has a wide range of applications in MI-EEG classification.

1. Introduction

BCI is a system that aims to establish a direct communication channel between the brain and computer [1,2] Researchers placed the electrodes on the scalp and collected electroencephalogram (EEG) noninvasively. BCI was adopted in many aspects, such as text typing systems [3,4], rehabilitation equipment [5,6], wheelchairs [7], etc. MI-EEG can be acquired easily, and researchers paid more attention to motor imagination recognition recently [8–10]. The imaginary movements of limbs and tongues [11,12] are the traditional tasks, and the recognition of the left and right-hand movement imagination is a research hotspot. The physiological mechanism of motor imagination contains event-related desynchronization (ERD) and event-related synchronization (ERS) [13,14], result showed that the energy of mu and β rhythm in the ipsilateral sensorimotor cortex increases, and the energy of mu and β rhythm in contralateral cortex decreases [15]. Recently EEG data acquisition generally uses the international 10–20 standard lead system, and EEG acquired through placing electrodes on the human scalp is non-invasive and cheap in large quantities [16]. However, EEG signals with small amplitude and low signal-to-noise ratio are submerged in noise and artifacts easily, and it is not conducive to the identification [17].

Researchers have proposed some classification methods by machine learning and convolutional neural networks (CNN) to recognize MI-EEG recently. Machine learning-based classification models [18,19] for the MI-EEG recognition include support vector machine (SVM), linear discriminant classifier (LDA), and so on. The feature extraction strategies [20,21] include common space pattern (CSP), principal component analysis (PCA), and so on. In 2017, Dong et al. proposed a hierarchical support vector machine (HSVM) algorithm to address an EEG-based four-class motor imagery classification task [22]. In 2021, Zhang et al. designed an integrated linear discriminant analysis (LDA) classifier and verified the effectiveness of the algorithm using the public datasets and the private EEG datasets including healthy subjects and stroke patients [23]. In 2021, Malan and Sharma designed a dual-tree complex wavelet transform to filter EEG signals

* Corresponding author at: College of Medical Engineering, Xinxiang Medical University, Xinxiang 453003, China.
E-mail address: yywzfb_bme@outlook.com (Y. Yu).

https://doi.org/10.1016/j.asoc.2022.109685
1568-4946/

into sub-bands, used CSP to extract spatial features from each sub-band, optimized feature vector by the supervised learning framework, and classified EEG signals using support vector machine (SVM) [24]. Machine learning-based classification models can achieve good classification accuracy. However, feature selecting and classifying need to be designed manually according to the characteristics of EEG signals, and it limited its wide application.

CNN has been applied to the recognition of MI-EEG [25,26], and they solved the problems of machine learning-based classification methods. The input data forms of the network model are time domain, time–frequency diagrams, and other data. In 2018, Lawhern et al. proposed an EEGNet and used the time domain of EEG signals as the model input to identify various BCI paradigms [27]. In 2021, Liu et al. designed an end-to-end convolutional neural network model (CNN-GRU) to complete the classification of EEG-based four-class tasks [28]. In 2020, Riyad et al. proposed Incep-EEGNet and applied it to the classification of MI-EEG [29]. MI-EEG is unclear in the time domain, and the classification accuracy of the time-domain EEG signals is low. MI-EEG has the obvious difference in the frequency domain, and the time–frequency transformation strategies such as continuous wavelet transform (CWT) [30,31] and short-time Fourier transform (STFT) [32,33] were adopted to obtain the time–frequency diagrams. In 2021, Keerthi et al. generated EEG spectrum images by Variational Mode Decomposition (VMD) and Short Time Fourier Transform (STFT) and classified them using CNN on public motor imagination datasets [34]. In 2018, Hu et al. proposed an EEG feature extraction strategy using Wavelet Transform (WT) and Short-Time Fourier Transform (STFT) and used the convolution neural network to address EEG-based two-class motor imagery classification task [35]. In 2020, Li et al. proposed a novel MI-EEG classification algorithm by combining CWT and a simplified convolutional neural network (SCNN). This model was tested on BCI Competition IV Dataset 2b [36]. In 2019, Xu et al. adopted a wavelet transform input to extract the features of the MI-EEG signal and designed a two-layer convolutional neural network to address the MI-EEG classification task [37]. In 2021, Xiao et al. used STFT and CMWT to preprocess the collected experimental data and designed the improved CNN network model to recognize EEG signals efficiently [38].

For the MI-EEG classification problem, feature extracting and classifier designing were crucial, and how to obtain the time–frequency diagrams is the key to the motor imagination classification method. However, researchers have not discussed the effect of wavelet parameters on the results by comparing the classification results of the different continuous wavelet transforms. To improve the classification accuracy, we proposed a novel MI-EEG classification method by combining Shannon complex wavelets and convolutional neural networks. First, we preprocessed the MI-EEG with EEGLAB by channel selection, frequency filter, and trial interception. Second, we used Shannon Complex wavelet as the time–frequency transformation strategy to calculate the time–frequency matrix. Finally, we used the improved Resnet to classify the time–frequency matrix and completed the MI-EEG recognition. BCI competition IV dataset 2b was tested to demonstrate the effectiveness of the proposed method. Classification accuracy and kappa values were adopted as evaluation metrics to demonstrate the superiority of the proposed method by comparing it with the state-of-the-art methods. We also discussed and optimized the parametric effects of wavelet wavelength and interception time on classification accuracy.

The key contributions of this study can be elaborated as the following three points:

(1) We proposed a novel MI-EEG classification method by combining Shannon Complex wavelet and convolutional neural networks.

(2) The classification accuracy and Kappa value by the proposed method improved by 2% and 0.04 than by the best classification method on BCI Competition IV Dataset 2b.

(3) We discussed and optimized the parameter influence on the classification accuracy.

The rest of this study is organized as follows: Section 2 presents the proposed method; Section 3 shows the experimental results and comparative analysis; Section 4 discusses the parameter influence; Section 5 concludes this study.

2. Method

In this study, we proposed a novel MI-EEG classification method by combining Shannon Complex wavelet and convolutional neural networks to improve classification accuracy. Fig. 1 shows the flow chart of this experiment. The proposed method contains three steps: (a) preprocess the original MI-EEG signal using the EEGLAB, (b) calculate the time–frequency matrix using Shannon Complex wavelet, (c) adopt the convolutional neural networks to classify time–frequency matrix, and complete the recognition of the MI-EEG. Firstly, we selected the C3 and C4 time-domain EEG signals as the processing data and filtered the original signals by the band-pass filter, and intercepted the trials. Secondly, we calculated the time–frequency matrix using Shannon Complex wavelet. Finally, we adopted the improved Resnet to classify the time–frequency matrix and completed the classification of left and right-hand motor imagination.

2.1. Data preprocessing

We completed the data preprocessing using EEGLAB toolbox. The preprocessing steps can be implemented as follows: (a) channel selecting, (b) frequency filter, and (c) trial interception. Firstly, the irrelevant channels were eliminated from the raw signals, and the C3 and C4 channels were retained. The C3 and C4 electrodes can represent the left and right sensory-motor regions of the brain. We compared the classification results using all channels with the C3 and C4 channels and concluded that the classification accuracy using all channels is not higher than that of C3 and C4 channels. We used the C3 and C4 signals to classifier the left and right-hand motor imagination in this study. Secondly, we found that the time–frequency diagrams are more efficient than the time-domain diagrams for the EEG-MI classification, so we used the time–frequency diagrams as the input of convolutional neural networks in this study. The 1–30 Hz frequency are important for the MI-EEG classification [15], and we used a 1–30 Hz band-pass filter to eliminate the noise and artifacts. Finally, we intercepted every trial of the EEG signals. Fig. 2 shows the preprocessing result of MI-EEG.

2.2. time–frequency transform

We adopted the continuous wavelet transform to calculate the time–frequency diagrams of MI-EEG and extracted mu and beta rhythms from the time–frequency diagrams. The continuous wavelet transform was described as follows

$$WT_x(c,d) = \frac{1}{\sqrt{|c|}} \int_{-\infty}^{+\infty} x(t)\, \psi^*\left(\frac{t-d}{c}\right) dt \tag{1}$$

where $\psi(t)$ is the fundamental wavelet, and $\psi_{c,d}(t)$ is a family of functions generated by the shift or expansion of fundamental wavelet, c is the scale factor, and d is the time shift. Time center and time span of the continuous wavelet can be calculated as follows:

$$t^* = \frac{\int_{-\infty}^{+\infty} t \left|\psi_{c,d}(t)\right|^2 dt}{\int_{-\infty}^{+\infty} \left|\psi_{c,d}(t)\right|^2 dt} \tag{2}$$

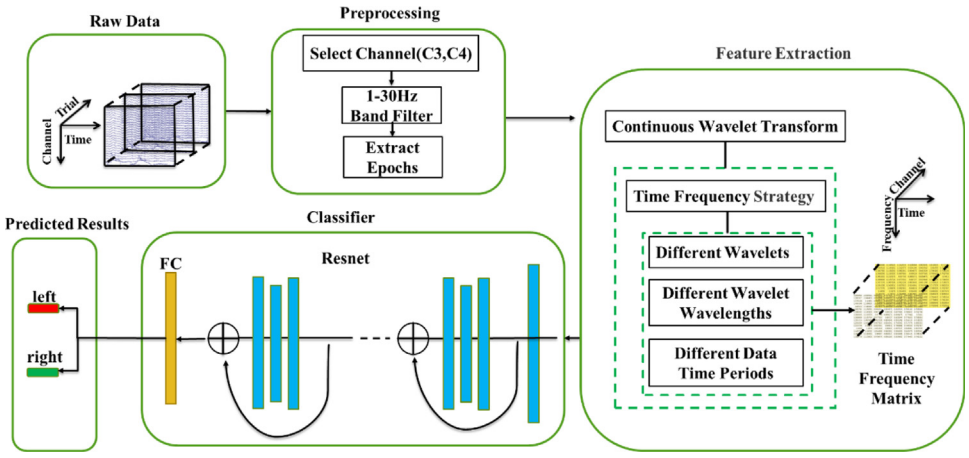

Fig. 1. The MI-EEG classification framework.

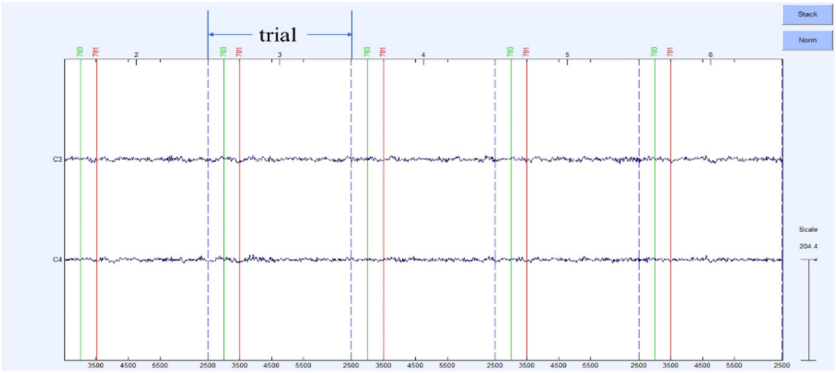

Fig. 2. C3 and C4 time-domain MI-EEG by the data processing strategy.

$$\Delta t = \left[\frac{\int_{-\infty}^{+\infty} (t - t^*)^2 \left| \psi_{c,d}(t) \right|^2 dt}{\int_{-\infty}^{+\infty} \left| \psi_{c,d}(t) \right|^2 dt} \right]^{\frac{1}{2}} \tag{3}$$

Central frequency and bandwidth of the continuous wavelet can be calculated as follows:

$$\omega^* = \frac{\int_{-\infty}^{+\infty} \omega \left| \hat{\psi}_{c,d}(\omega) \right|^2 d\omega}{\int_{-\infty}^{+\infty} \left| \hat{\psi}_{c,d}(\omega) \right|^2 d\omega} \tag{4}$$

$$\Delta\omega = \left[\frac{\int_{-\infty}^{+\infty} (\omega - \omega^*)^2 \left| \hat{\psi}_{c,d}(\omega) \right|^2 d\omega}{\int_{-\infty}^{+\infty} \left| \hat{\psi}_{c,d}(\omega) \right|^2 d\omega} \right]^{\frac{1}{2}} \tag{5}$$

The different definitions of the continuous wavelet can generate the different wavelet transform. In this study, we compared the three different wavelets and adopted Shannon Complex wavelet to extract the local and global time–frequency features of MI-EEG.

Morlet wavelet is a single frequency complex sinusoidal function under Gaussian envelope. It can be calculated by formula (6)

$$W_{morl}(t) = e^{-(t^2/2)} \cos(5t) \tag{6}$$

Complex morlet wavelet is a non-orthogonal wavelet without the scale function. It has a good localization in time and frequency, and it can be calculated by formula (7)

$$W_{cmor}(t) = \frac{1}{\sqrt{\pi B}} e^{2i\pi Ct} e^{-(t^2/B)} \tag{7}$$

Shannon wavelet is a real wavelet, and it can be described as follows

$$W(t) = \frac{\sin(\pi(t - 1/2)) - \sin(2\pi(t - 1/2))}{\pi(t - 1/2)} \tag{8}$$

Shannon Complex wavelet is a non-orthogonal wavelet. It has an infinite support width, and it can be calculated by formula (9)

$$W_{shan}(t) = \sqrt{B} \frac{\sin(\pi Bt)}{\pi Bt} e^{2i\pi Ct} \tag{9}$$

where B is the bandwidth and C is the center frequency.

2.3. Classification model

In this study, we improved the standard Resnet [39] as the MI-EEG classification model. The improved classification network model is shown in Fig. 3. Fig. 3(a) is the improved Resnet, and Fig. 3(b) and (c) are the implementation units of the "conv_block" and "identity_block". The EEG time signal is the C3 and C4, and the interception time is 2.5–7 s. The sampling data is 1125, and the energy values of the EEG time signal were calculated and divided into 50 parts from 1 to 30 Hz linearly. The size of input data is 50 × 1125 × 2, and it was shown in Fig. 3(a). The improved Resnet model has "identity_block" and "conv_block" units. The uniform distribution initialization strategy was adopted in the convolution layer, and the random number was set to zero. The input and output sizes of the "identity_block" are the same, and the multiple "identity" blocks can be connected. The input and output sizes of the "conv_block" are different, and they can change the dimension of the feature maps. The improved Resnet

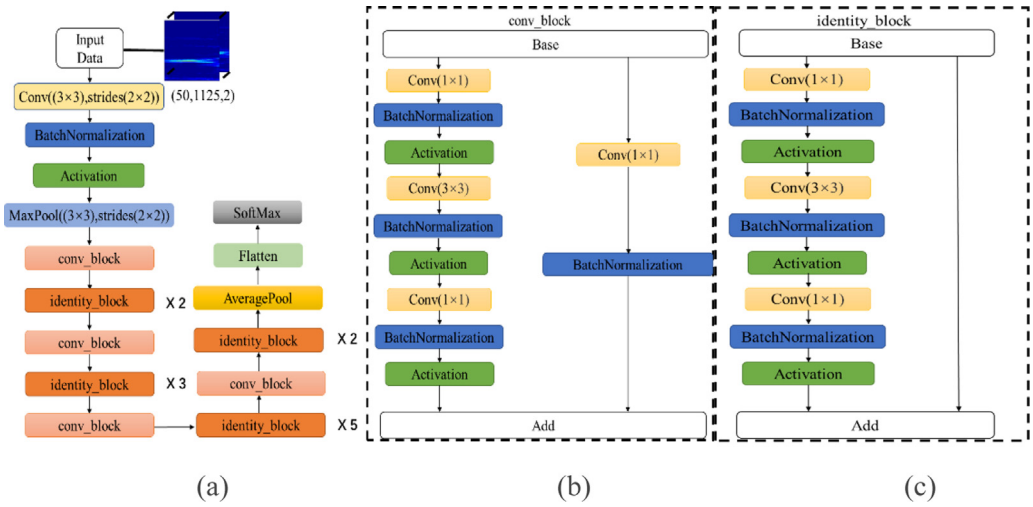

Fig. 3. The classification network model (a) is the improved Resnet, (b) is the "conv_block" unit, and (c) is the "identity_block" unit.

has 4 "conv_block" and 12 "identity_block" units. The model parameters were set as follows: the convolution core size of the first convolution layer was set to 3 × 3. The pooling kernel size of the average pooling layer is 2 × 2. The strides of the second, third and fourth layers of the "conv_block" are 1 × 1, 2 × 2, and 2 × 2, respectively. The categorical cross-entropy (CCS) was used as the loss function, and the stochastic gradient descent (SGD) was applied to minimize this loss function in this study. The k-fold cross-validation strategy was utilized with k set to 10, and 10 percent of training trials were used as the validation set. In this study, the learning rate adjustment was adopted, and the parameters were set as follows: the initial learning rate is set to 0.01, the scaling factor was set to 0.2, the minimum learning rate is 1e−7, and the patience was set to 5. In the training process, the batch-processing strategy was adopted, the batch size was set to 16, and the epoch was set to 50.

3. Result

All experiments were conducted in NVIDIA GTX2080Ti and Intel® Xeon(R) CPU E5-2578v3@2.5 GHz with 64G RAM. The operating system is Ubuntu 18.04.5 LTS.

In this study, we selected a public motor imagination dataset (BCI Competition IV Dataset 2b) to validate the effectiveness of the proposed method. The dataset was acquired from nine subjects at electrodes C3, Cz, and C4 with a sampling frequency of 250 Hz. Each subject participated in five sessions, and the last two sessions were selected as the experimental data. The experimental diagram of every trial is shown in Fig. 4. When a trial starts, a gray face label appears on the screen. At 2 s, the experimental device emits a short beep to remind the subjects to be ready to start the experiment. From 3 to 7.5 s, the subjects begin to imagine the movement direction of the gray face (left or right), depending on the cue. If the gray face is in the same direction as the cue, a green smiling face will appear on the screen; otherwise, a red sad face will appear. At 7.5 s, the cue disappears the screen becomes blank, and then start the next test after a random interval of 1 to 2 s. The interception time of each trial is from 2.5 to 7 s, and the data point of each trial is 1125. There are 80 trials of each type in each session, and there are 320 trials used in this study.

3.1. Results of the proposed method

We tested this proposed method on BCI Competition IV Dataset 2b to prove the effectiveness of the proposed method, and the parameters were set as follows: Shannon Complex wavelet was adopted to calculate the time–frequency matrix of C3 and C4 channels, and wavelet wavelength was set to −0.5–0.5 s. The intercept time of each trial was set to 2.5–7 s.

The time–frequency diagrams by Shannon Complex wavelet were shown in Fig. 5. Fig. 5(a) is the time–frequency diagram of the C3 channel by right-hand movement imagination, and Fig. 5(b) is the time–frequency diagram of the C3 channel by left-hand movement imagination. The classification accuracy is shown in Table 1. The average classification accuracy is 0.852, and the result demonstrated the effectiveness of the proposed method.

3.2. Comparison with the state-of-the-art MI-EEG classification methods

We compared the classification result of the state-of-the-art MI-EEG classification methods to demonstrate the superiority of this proposed method. In this study, we adopted the following state-of-the-art methods: Liu et al. proposed the classification method by combining Continuous wavelet transform (CWT) and a simplified convolution of neural network (SCNN) to complete the classification of MI-EEG tasks, which was shorted as CWT-SCNN [36]. Zhu et al. proposed a separated channel convolutional network to encode the multi-channel data, concatenated the encoded features, and performed the final MI-EEG task recognition, which was shorted as CSP-SCNN [40]. Tabar et al. proposed a new deep network by combining CNN and SAE to classify MI-EEG, which was shorted as CNN-SAE [41]. Dai et al. proposed an MI-EEG classification framework combining convolutional neural network (CNN) architecture with Variational Autoencoder (VAE), which was shorted as CNN-VAE [42]. Chen et al. proposed a deep learning framework and used the result of the time–frequency image subtraction of the MI-EEG C3 and C4 channels signals as the input of the classifier, which was shorted as IS-CBAM-CNN [8]. Lawhern et al. proposed a compact convolutional neural network for EEG-based Brain–Computer Interfaces, which was shorted EEGNet [27].

All comparative experiments are tested on BCI Competition IV Dataset 2b, and the training processing was the 10-fold cross-validation, and classification accuracy and kappa value were adopted as the evaluation metrics. Kappa value can measure the classification accuracy and eliminate the influence of the random classification [41], and it can be calculated by the formula (10)

$$kappa = \frac{p_0 - p_e}{1 - p_e} \tag{10}$$

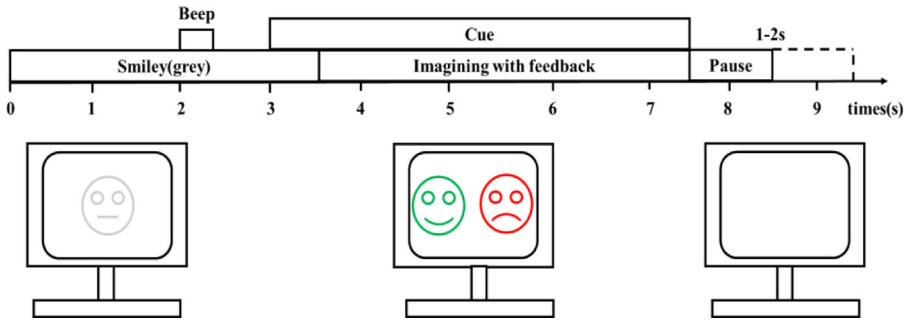

Fig. 4. Experimental diagram of motor imagination.

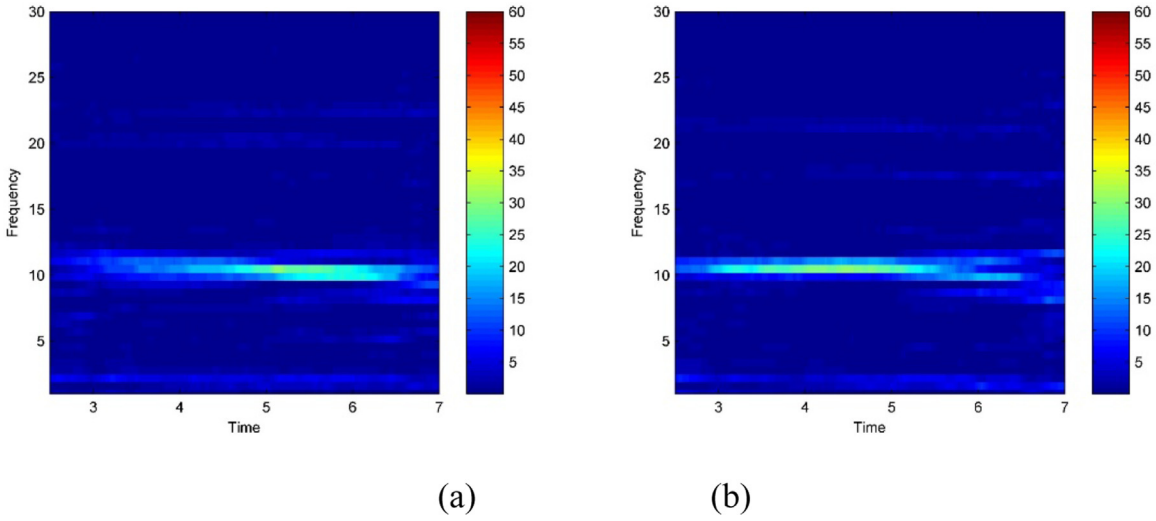

Fig. 5. Time–frequency diagrams by Shannon Complex wavelet.

Table 1
Classification accuracy of different subject by the proposed method.

Subject	1	2	3	4	5	6	7	8	9	Average accuracy
Accuracy	0.781	0.643	0.647	0.972	0.978	0.931	0.859	0.925	0.928	0.852

where p_0 is the subject's classification accuracy, and p_e is the random classification accuracy, which was set to 0.5 [36].

The MI-EEG classification results by the state-of-the-art methods are shown in Table 2, and it showed that the classification accuracy is 0.852 the kappa value is 0.704, and that they are the highest in the state-of-the-art methods. It demonstrated the superiority of this proposed method. The classification accuracy and kappa value by the proposed method are higher than the best in Table 2 by 2% and 0.04, respectively.

The input form of EEGNet is the time-domain diagrams, and the result using EEGNet showed that the classification accuracy is lower than that by combining the continuous wavelet transform and convolutional neural networks. This is because there are no obvious differences in the left and right-hand MI-EEG time-domain signals, and it is difficult to classifier the MI-EEG efficiently using the time-domain signal for the convolutional neural networks. The classification method by combining the continuous wavelet transform and convolutional neural networks is mainstream, which used the time–frequency diagrams as the input of convolutional neural networks, and the time–frequency matrix was used as the input of the proposed method.

3.3. Comparison with the state-of-the-art CWT

Several classification methods by combining the different continuous wavelet transform and convolutional neural networks have been proposed recently. The input form of network models was time–frequency diagrams, and the time–frequency diagrams by the different wavelet transform methods have a great influence on the classification results. Morlet wavelet and complex morlet wavelet as the time–frequency transform strategies were applied to obtain the time–frequency diagrams, and the classification accuracy was compared in the literature [30]. We proposed the Shannon Complex wavelet as the time–frequency transform to obtain the time–frequency diagram in this study. The time–frequency diagrams by the different continuous wavelet transform strategies are shown in Fig. 6. The left column is the time–frequency diagram of the C3 channel by right-hand movement imagination, and the right column is the time–frequency diagram of the C3 channel by left-hand movement imagination.

Table 2
Classification results of MI-EEG by the State-of-the-art methods.

Method	Classification accuracy	Kappa value
CWT-SCNN [36]	0.832	0.664
CSP-SCNN [40]	0.730	0.460
CNN-SAE [41]	0.751	0.502
CNN-VAE [42]	0.782	0.564
IS-CBAM-CNN [8]	0.796	0.592
EEGNet [27]	0.745	0.491
Proposed method	0.852	0.704

Table 3
Classification results of MI-EEG by the different continuous wavelet transform strategies.

Subject	Complex morlet wavelet		Morlet wavelet		Shannon wavelet		Shannon Complex wavelet	
	Classification accuracy	Kappa value	Classification accuracy	Kappa value	Classification accuracy	Kappa value	Classification accuracy	Kappa value
1	0.781	0.562	0.716	0.432	0.628	0.256	0.781	0.562
2	0.629	0.258	0.639	0.278	0.657	0.314	0.643	0.286
3	0.631	0.262	0.641	0.282	0.659	0.318	0.647	0.294
4	0.969	0.938	0.978	0.956	0.934	0.868	0.972	0.944
5	0.978	0.956	0.978	0.956	0.966	0.932	0.978	0.956
6	0.900	0.800	0.888	0.776	0.734	0.468	0.931	0.862
7	0.806	0.612	0.859	0.718	0.691	0.382	0.859	0.718
8	0.941	0.882	0.941	0.882	0.894	0.788	0.925	0.850
9	0.888	0.776	0.894	0.788	0.813	0.626	0.928	0.856
Average	0.836	0.672	0.837	0.674	0.775	0.550	0.852	0.704

Fig. 6(a–b) is the time–frequency diagram by complex morlet wavelet, Fig. 6(c–d) is the time–frequency diagram by Shannon Complex wavelet, Fig. 6(e–f) is the time–frequency diagram by Shannon wavelet, and Fig. 6(g-h) is the time–frequency diagram by morlet wavelet. We concluded that the time–frequency diagrams were different by the different continuous wavelet transform strategies and that they had a great influence on the classification results.

We discussed the influence of different wavelet transform methods on the classification results to demonstrate the superiority of the Shannon Complex wavelet transform strategy. Classification accuracy and kappa value of MI-EEG by the different continuous wavelet transform strategies were shown in Table 3. The result showed that the average accuracy and kappa value by the Shannon Complex wavelet are 0.852 and 0.704, respectively, and it is higher than that by the morlet wavelet, complex morlet wavelet, and Shannon wavelet. We can conclude that the Shannon Complex wavelet as the time–frequency transform strategy is the best for the MI-EEG recognition in the different continuous wavelet transform methods.

3.4. Extended application

We used BCI Competition III (2005) dataset IIIb (BCI III IIIb), BCI Competition III (2005) dataset IVa (BCI III IVa) [43], and BCI Competition II (2003) dataset III (BCI II III) to test the application range of this proposed method. The experimental paradigm of these datasets is the same as BCI Competition IV Dataset 2b, and they are all left–right motor imagery. The experimental results are shown in Table 4. For BCI III IIIb, there are three subjects, and the mean classification accuracy and mean kappa values are 0.929 and 0.857, respectively. For BCI III IVa, there are five subjects, and the mean classification accuracy and mean kappa values are 0.918 and 0.837, respectively. For BCI III III, there is one subject, and the mean classification accuracy and mean kappa values are 0.993 and 0.986, respectively. It demonstrated that this method has a wide range of applications in MI-EEG classification.

Table 4
Evaluation results of the proposed method on other datasets.

	Subject	Classification accuracy	Kappa value
BCI III IIIb	O3	0.935	0.870
	S4	0.944	0.888
	X11	0.907	0.814
	Average	0.929	0.857
BCI III IVa	aa	0.917	0.834
	al	0.964	0.928
	av	0.889	0.778
	aw	0.893	0.786
	ay	0.929	0.858
	Average	0.918	0.837
BCI II III	1	0.993	0.986

Table 5
Classification accuracy of MI-EEG by the Shannon Complex wavelet with the different wavelet wavelength setting.

Subject	Classification accuracy			
	−0.2–0.2 s	−0.5–0.5 s	−0.7–0.7 s	−1–1 s
1	0.744	0.781	0.766	0.784
2	0.636	0.643	0.668	0.621
3	0.641	0.647	0.631	0.675
4	0.978	0.972	0.991	0.988
5	0.988	0.978	0.975	0.966
6	0.897	0.931	0.866	0.888
7	0.859	0.859	0.853	0.847
8	0.934	0.925	0.922	0.931
9	0.906	0.928	0.913	0.906
Average	0.843	0.852	0.843	0.845

4. Discussion

4.1. Discussion of parameter setting

In this study, wavelet wavelength and trial time duration are the parameters, and we discussed the influence of parameters on the experimental results and optimize the parameter setting.

Shannon Complex wavelet was adopted as the time–frequency transform strategy, and wavelet wavelength is the parameter of the proposed method. We discussed the influence of wavelet wavelength on the classification accuracy, and the wavelet wavelength parameter was set to −0.2–0.2 s, −0.5–0.5 s, −0.7–0.7 s, and −1–1 s respectively, from left to right. Classification accuracy is shown in Table 5, and the result showed that when the wavelet wavelength was set to −0.5–0.5 s the average accuracy is 0.852, and it is the highest in the different wavelet wavelengths. In this study, the wavelet wavelength was set to −0.5–0.5 s.

We discussed the influence of interception time on the classification accuracy, and the interception time parameter was set to 2.5–7 s, 3–7.5 s, and 3.5–8 s respectively. The result is shown in Table 6, and it showed that when the interception time was set to 2.5–7 s the average accuracy is 0.852 and that it is the highest. This result is consistent with those in the literature [41]. In this study, the interception time was set to 2.5–7 s for the public BCI Competition IV Dataset 2b.

4.2. Discussion of network depth

The proposed method has 4 “conv_block” and 12 “identity_block” units, and Table 7 shows the influence of adding “conv_block” and “identity_block” units on classification results. From Table 7, we can see that the model parameters and training time increase as the depth of the model increases, but the average accuracy of the model does not increase obviously. We

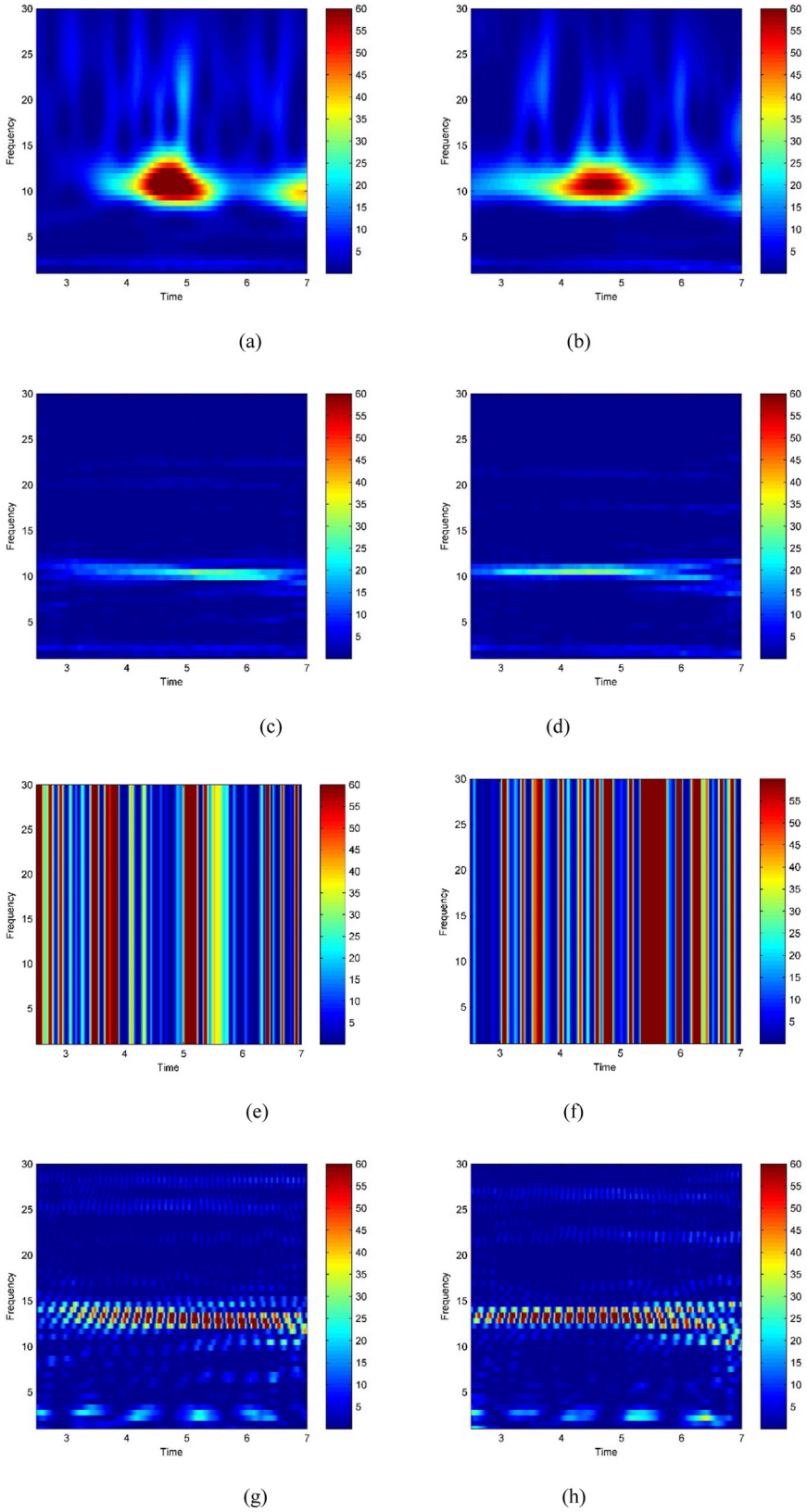

Fig. 6. Time–frequency diagrams by the different continuous wavelets.

Table 6
Classification accuracy of MI-EEG by the different interception time setting.

Subject	Classification accuracy		
	2.5–7 s	3–7.5 s	3.5–8 s
1	0.782	0.788	0.794
2	0.643	0.639	0.604
3	0.647	0.650	0.641
4	0.972	0.991	0.983
5	0.978	0.984	0.975
6	0.931	0.900	0.866
7	0.859	0.847	0.850
8	0.925	0.941	0.934
9	0.928	0.909	0.925
Average	0.852	0.850	0.841

Table 7
Influence of network depth on classification results.

Conv_block	Identity_block	Average accuracy	Model parameters (/million)	Training time (/h)
4	12	0.852	23.9	8.75 h
5	14	0.843	24.2	10.0 h
5	16	0.845	33.5	10.3 h
5	18	0.849	33.7	11.3 h
6	14	0.843	33.0	11.5 h
6	16	0.849	41.6	12.5 h
6	18	0.851	42.1	13.8 h

concluded that the proposed method has the highest average accuracy and the least number of network parameters and training time when the classification model has 4 “conv_block” and 12 “identity_block” units.

5. Conclusion

In this study, we proposed a novel classification method by combining Shannon Complex wavelet and Convolutional neural networks to improve the classification accuracy. Firstly, we completed the MI-EEG preprocessing by the EEGLAB by channel selection, frequency filter, and trial interception. Secondly, we calculate the time–frequency matrix of the time-domain MI-EEG using Shannon Complex wavelet. Finally, we adopted the improved Resnet to classifier the time–frequency matrix and completed the MI-EEG recognition. We used BCI competition IV dataset 2b as a public motor imagination dataset to prove the validation of the proposed method. We adopted classification accuracy and kappa value as evaluation metrics to prove the superiority of the proposed method by comparing it with state-of-the-art methods. Results showed that the average classification accuracy and kappa value are 0.852 and 0.704, respectively, and that they are the highest in the state-of-the-art methods. We also discussed and optimized the parameter influence of wavelet wavelength and interception time on the classification accuracy. This method can effectively improve the classification result of MI-EEG, and it has clinical application value.

CRediT authorship contribution statement

Chang Wang: Revision - first draft, Writing and experimental guidance. **Yang Wu:** Get the results of the experiment, Write the first draft. **Chen Wang:** Auxiliary drawing and sorting results. **Yu Zhu:** Find data, Filter data and draw pictures. **Chong Wang:** Guide article writing and error correction. **Yanxiang Niu:** Programming guidance and error correction. **Zhenpeng Shao:** Auxiliary modification of articles. **Xudong Gao:** Auxiliary modification chart. **Zongya Zhao:** Programming guidance and result correction. **Yi Yu:** Supervision, Project administration, Writing – review & editing.

Declaration of competing interest

The authors declare that they have no known competing financial interests or personal relationships that could have appeared to influence the work reported in this paper.

Data availability

The authors do not have permission to share data.

Acknowledgments

This work was supported by the Open Project Program of the Third Affiliated Hospital of Xinxiang Medical University (No. KFKTYB202109), and the Research Project on educational and teaching reform of Xinxiang Medical University, China (No. 2021-XYJG-32). The scientific research and innovation support plan of Xinxiang Medical University, China in 2021 (No. YJSCX202120Z).

References

[1] X. Zhang, et al., A survey on deep learning-based non-invasive brain signals:Recent advances and new frontiers, 2020, arXiv:190504149 Cs Eess Q-Bio.
[2] K. Renuga Devi, H. Hannah Inbarani, Neighborhood based decision theoretic rough set under dynamic granulation for BCI motor imagery classification, J. Multimodal User Interfaces 15 (2021) 301–321.
[3] X. Zhang, et al., Converting your thoughts to texts: Enabling brain typing via deep feature learning of EEG signals, 2017, arXiv:170908820 Cs.
[4] I. Raza, EmoWrite- A Sentiment Analysis-Based Thought to Text Conversion-2. 26.
[5] S. Bhattacharyya, A. Konar, D.N. Tibarewala, Motor imagery, P300 and error-related EEG-based robot arm movement control for rehabilitation purpose, Med. Biol. Eng. Comput. 52 (2014) 1007–1017.
[6] A.S. Royer, A.J. Doud, M.L. Rose, B. He, EEG control of a virtual helicopter in 3-dimensional space using intelligent control strategies, IEEE Trans. Neural Syst. Rehabil. Eng. 18 (2010) 581–589.
[7] H.-C. Chou, N. Prataksita, Y.-T. Lin, C.-H. Kuo, P300 and motor imagery based brain-computer interface for controlling Wheelchairs1, J. Med. Devices 8 (2014) 030906.
[8] Z. Chen, Y. Wang, Z. Song, Classification of motor imagery electroencephalography signals based on image processing method, Sensors 21 (2021) 4646.
[9] F. Pichiorri, et al., Brain-computer interface boosts motor imagery practice during stroke recovery: BCI and Motor Imagery, Ann. Neurol. 77 (2015) 851–865.
[10] J. Kevric, A. Subasi, Comparison of signal decomposition methods in classification of EEG signals for motor-imagery BCI system, Biomed. Signal Process. Control 31 (2017) 398–406.
[11] M.-A. Li, J.-F. Han, L.-J. Duan, A novel MI-EEG imaging with the location information of electrodes, IEEE Access 8 (2020) 3197–3211.
[12] V. Morash, O. Bai, S. Furlani, P. Lin, M. Hallett, Classifying EEG signals preceding right hand, left hand, tongue, and right foot movements and motor imageries, Clin. Neurophysiol. 119 (2008) 2570–2578.
[13] V.K. Benzy, A.P. Vinod, R. Subasree, S. Alladi, K. Raghavendra, Motor imagery hand movement direction decoding using brain computer interface to aid stroke recovery and rehabilitation, IEEE Trans. Neural Syst. Rehabil. Eng. 28 (2020) 3051–3062.
[14] Z. Tang, et al., A brain-machine interface based on ERD/ERS for an upper-limb exoskeleton control, Sensors 16 (2016) 2050.
[15] G. Pfurtscheller, Ch. Neuper, D. Flotzinger, M. Pregenzer, EEG-based discrimination between imagination of right and left hand movement, Electroencephalogr. Clin. Neurophysiol. 103 (1997) 642–651.
[16] E. Bou Assi, D.K. Nguyen, S. Rihana, M. Sawan, Towards accurate prediction of epileptic seizures: A review, Biomed. Signal Process. Control 34 (2017) 144–157.
[17] Hu, Application of energy entropy in motor imagery EEG classification, Int. J. Digit. Content Technol. Its Appl. 3 (2009).
[18] C.-C. Chang, C.-J. Lin, LIBSVM: A library for support vector machines, ACM Trans. Intell. Syst. Technol. 2 (2011) 1–27.
[19] C. Vidaurre, M. Kawanabe, P. von Bünau, B. Blankertz, K.R. Müller, Toward unsupervised adaptation of LDA for brain–computer interfaces, IEEE Trans. Biomed. Eng. 58 (2011) 587–597.

[20] C. Gouy-Pailler, M. Congedo, C. Brunner, C. Jutten, G. Pfurtscheller, Nonstationary brain source separation for multiclass motor imagery, IEEE Trans. Biomed. Eng. 57 (2010) 469–478.
[21] C. Brunner, M. Naeem, R. Leeb, B. Graimann, G. Pfurtscheller, Spatial filtering and selection of optimized components in four class motor imagery EEG data using independent components analysis, Pattern Recognit. Lett. 28 (2007) 957–964.
[22] E. Dong, et al., Classification of multi-class motor imagery with a novel hierarchical SVM algorithm for brain–computer interfaces, Med. Biol. Eng. Comput. 55 (2017) 1809–1818.
[23] Y. Zhang, et al., Boosting-LDA algriothm with multi-domain feature fusion for motor imagery EEG decoding, Biomed. Signal Process. Control 70 (2021) 102983.
[24] N.S. Malan, S. Sharma, Motor imagery EEG spectral-spatial feature optimization using dual-tree complex wavelet and neighbourhood component analysis, 2021, http://dx.doi.org/10.1016/j.irbm.2021.01.002, IRBM S1959031821000038.
[25] A. Sors, S. Bonnet, S. Mirek, L. Vercueil, J.-F. Payen, A convolutional neural network for sleep stage scoring from raw single-channel EEG, Biomed. Signal Process. Control 42 (2018) 107–114.
[26] T. Tezuka, et al., Real-time, automatic, open-source sleep stage classification system using single EEG for mice, Sci. Rep. 11 (2021) 11151.
[27] V.J. Lawhern, et al., EEGNet: A compact convolutional network for EEG-based brain-computer interfaces, J. Neural Eng. 15 (2018) 056013.
[28] J. Liu, F. Ye, H. Xiong, Multi-class motor imagery EEG classification method with high accuracy and low individual differences based on hybrid neural network, J. Neural Eng. 18 (2021) 0460f1.
[29] M. Riyad, M. Khalil, A. Adib, Incep-EEGNet: A ConvNet for motor imagery decoding, in: A. El Moataz, D. Mammass, A. Mansouri, F. Nouboud (Eds.), Image and Signal Processing, Vol. 12119, Springer International Publishing, 2020, pp. 103–111.
[30] M. Li, J. Han, J. Yang, Automatic feature extraction and fusion recognition of motor imagery EEG using multilevel multiscale CNN, Med. Biol. Eng. Comput. 59 (2021) 2037–2050.
[31] M. Sadat Shahabi, A. Shalbaf, A. Maghsoudi, Prediction of drug response in major depressive disorder using ensemble of transfer learning with convolutional neural network based on EEG, Biocybern. Biomed. Eng. 41 (2021) 946–959.
[32] K.-W. Ha, J.-W. Jeong, Motor imagery EEG classification using capsule networks, Sensors 19 (2019) 2854.
[33] M. Sameer, B. Gupta, Time–frequency statistical features of delta band for detection of epileptic seizures, Wirel. Pers. Commun. 122 (2022) 489–499.
[34] K. Keerthi Krishnan, K.P. Soman, CNN based classification of motor imaginary using variational mode decomposed EEG-spectrum image, Biomed. Eng. Lett. 11 (2021) 235–247.
[35] Y. Hu, L. Wang, W. Fu, EEG feature extraction of motor imagery based on WT and STFT, in: 2018 IEEE International Conference on Information and Automation, ICIA, IEEE, 2018, pp. 83–88, http://dx.doi.org/10.1109/ICInfA.2018.8812377.
[36] F. Li, et al., A novel simplified convolutional neural network classification algorithm of motor imagery EEG signals based on deep learning, Appl. Sci. 10 (2020) 1605.
[37] B. Xu, et al., Wavelet transform time-frequency image and convolutional network-based motor imagery EEG classification, IEEE Access 7 (2019) 6084–6093.
[38] X. Xiao, Y. Fang, Motor imagery EEG signal recognition using deep convolution neural network, Front. Neurosci. 15 (2021) 655599.
[39] J. Zhang, B. Xie, X. Wu, R. Ram, D. Liang, Classification of diabetic retinopathy severity in fundus images with DenseNet121 and ResNet50, 2021, arXiv:210808473 Cs Eess.
[40] X. Zhu, et al., Separated channel convolutional neural network to realize the training free motor imagery BCI systems, Biomed. Signal Process. Control 49 (2019) 396–403.
[41] Y.R. Tabar, U. Halici, A novel deep learning approach for classification of EEG motor imagery signals, J. Neural Eng. 14 (2017) 016003.
[42] M. Dai, D. Zheng, R. Na, S. Wang, S. Zhang, EEG classification of motor imagery using a novel deep learning framework, Sensors 19 (2019) 551.
[43] T. Ölmez, Classification of Motor Imagery EEG Signals by Using a Divergence Based Convolutional Neural Network. 35.